ResearchGate

See discussions, stats, and author profiles for this publication at: https://www.researchgate.net/publication/230993978

Phase-Locked Modes, Phase Transitions and Component Oscillators in Biological Motion

Article *in* Physica Scripta · November 2006

DOI: 10.1088/0031-8949/35/1/020

CITATIONS
136

READS
187

4 authors:

Scott Kelso
Florida Atlantic University
329 PUBLICATIONS **27,068** CITATIONS
SEE PROFILE

Gregor Schöner
Ruhr-Universität Bochum
297 PUBLICATIONS **14,574** CITATIONS
SEE PROFILE

John Scholz
University of Delaware
111 PUBLICATIONS **7,867** CITATIONS
SEE PROFILE

Hermann Haken
Universität Stuttgart
590 PUBLICATIONS **22,809** CITATIONS
SEE PROFILE

Some of the authors of this publication are also working on these related projects:

Active Leg Exoskeleton (ALEX2) View project

Learning Dynamics View project

All content following this page was uploaded by Scott Kelso on 21 January 2014.

The user has requested enhancement of the downloaded file.

Physica Scripta. Vol. 35, 79–87, 1987.

Phase-Locked Modes, Phase Transitions and Component Oscillators in Biological Motion

J. A. S. Kelso*†, G. Schöner*, J. P. Scholz† and H. Haken‡

*Center for Complex Systems, Florida Atlantic University, Boca Raton, FL 33431, U.S.A.; †Haskins Laboratories, New Haven, CT 06511, U.S.A.
‡Institut für theoretische Physik, Universität Stuttgart, Stuttgart, F.R. of Germany

Received August 29, 1986; accepted September 10, 1986

Abstract

We review the results of joint experimental and theoretical work on coordinated biological motion demonstrating the close alliance between our observations and other nonequilibrium phase transitions in nature (e.g., the presence of critical fluctuations, critical slowing down). Order parameters are empirically determined and their (low-dimensional) dynamics used in order to explain specific pattern formation in movement, including stability and loss of stability leading to behavioral change, phase-locked modes and entrainment. The system's components and their dynamics are identified and it is shown how these may be coupled to produce observed cooperative states. This "phenomenological synergetics" approach is minimalist and operational in strategy, and may be used to understand other systems (e.g., speech), other levels (e.g., neural) and the linkage among levels. It also promotes the search for additional forms of order in multi-component, multi-stable systems.

1. Introduction

One may well ask: What role might the theoretical and experimental study of coordinated movement play in a conference on the Physics of Structure and Complexity? There are at least two reasons for its inclusion. One is that the movements of animals and people are *ordered spatiotemporal structures* that arise in a system composed of very many neural, muscular and metabolic components that operate on different time scales. The order is such that we are often able to classify it, like the gaits of a horse, for example, or the limited number of basic sounds (the so-called phonemes), that are common to all languages. Structure, then, emerges from complexity in a fashion reminiscent of the spontaneous formation of structure in open, nonequilibrium systems (e.g., [1, 2]).

A second reason for allying movement to a physics of complexity is that biological systems are *behaviorally complex*. They are multifunctional in the sense that they are capable of producing a wide variety of behaviors often using the same set of anatomical components (e.g., speaking and chewing). In certain cases, this behavioral complexity may, nevertheless, have a common basis. For example, common to many creatures – vertebrate and invertebrate – is the ability to generate *rhythmical* acts such as walking, flying and feeding. Since rhythmic behaviors are supported by such a diversity of neural processes, they may be a good starting place to look for laws underlying behavioral complexity.

How then is order in biological coordination to be characterized? Ideally, one would like to have a model system that affords the analysis of pattern and change in pattern, both in terms of experimental data and theoretical tools. Here we describe an ongoing program of research in which theory and experiment have gone (literally), hand in hand, and whose main aims are to understand: (1) The formation of ordered, cooperative states in biological motion; (2) The stability of these observed states; and (3) The conditions that give rise to switching cooperative states. Although our experimental paradigms are concerned with movement control, we believe they might also offer a window into stability and change in general, in a biological system whose real-time behavior can be monitored continuously. We start with some basic facts obtained by ourselves and others. Then we map these observations onto an explicit model that in turn predicts additional aspects which are also studied.

2. Phase transitions in biological movement

Our experiments deal with rhythmical finger (or hand) movements in human subjects. We monitor the kinematic characteristics of these movements using infrared light-emitting diodes attached to the moving parts. The output of these diodes is detected by a *Selspot* optoelectronics camera systems. On occasion, we also record from relevant muscles using surface or fine-wire platinum electrodes as the occasion demands (see, e.g., [3]). Thus the behavioral phenomena can be examined at both kinematic and neuromuscular levels. All data are recorded on a 14-channel FM recorder for later off-line digitization at 200 samples/sec., and consequent computer analysis.

Following a paradigm introduced by Kelso [4; 5], subjects oscillate their index fingers bilaterally in the transverse plane (i.e., abduction-adduction) in one of two patterns (in-phase or anti-phase). In the former pattern, homologous muscles contract simultaneously; in the latter, the muscles contract in an alternating fashion. Using a pacing metronome, the frequency of oscillation is systematically increased from 1.25 Hz to 3.50 Hz in 0.25 Hz steps every 4 sec (see [3, 6].

Data from the last 3 sec of each frequency plateau (600 data samples) are used for the calculation of averages to secure stationarity. Figure 1 shows a time series when the system is prepared initially in the anti-phase mode. Obviously, at a certain critical frequency the subject switches spontaneously into the in-phase mode. No such switching occurs when the subject starts in the in-phase mode. Thus, while there are two stable patterns for low frequency values, only one pattern remains stable as frequency is scaled beyond a critical region. This transition behavior can be monitored by calculating the relative phase between the two fingers. A *point estimate* of relative phase is the latency of one finger with respect to the other finger's cycle, as determined from peak-to-peak displacement. A *continuous estimate* of relative phase (i.e., at the sampling rate of 200 Hz) can be obtained from the phase plane trajectories of both fingers. (The velocities are obtained by a central difference numerical differentiation procedure). Normalizing the finger oscillations to the unit circle, the phases of the individual fingers can be obtained

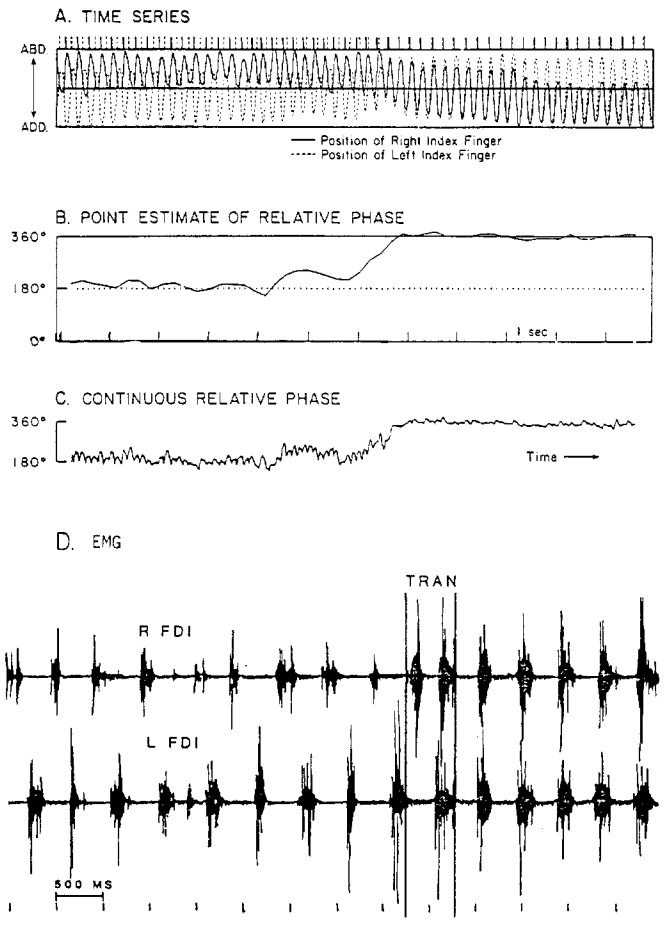

Fig. 1. (A) Time series of left and right finger position. (B) Point estimate of the relative phase. (C) Continuous relative phase. (D) The EMG record of FDI from right and left index finger movements (see text for details).

simply from the arctan $(\dot{x}/x)$ if x is normalized finger position (see [7]). Relative phase is then just the difference between these individual phases. In Figure 1 the relative phase fluctuates before the transition and stabilizes thereafter (cf. [3, 5, 6]).

3. Dynamical modeling

In order to understand temporal order and the observed change of such order in terms of dynamics, we need to address the following questions: First, what are the essential variables (order parameters) and how can their dynamics be characterized? Second, what are the 'control' parameters, that move the system through its collective states? Third, given a model, what new observations does the model predict? In a first step, relative phase, ϕ may be considered a suitable collective variable that can serve as order parameter. The reasons are as follows: (1) relative phase, ϕ characterizes the observed, coordinative modes; (2) ϕ changes abruptly at the transition and is only weakly dependent on parameters outside the transition; (3) ϕ has very simple dynamics in which the ordered phase-locked states are characterized by fixed point attractors. Since the prescribed frequency of oscillation, manipulated during the experiment, is followed very closely, frequency does not appear to be system dependent and can be considered the control parameter.

It is thus possible to determine the dynamics of ϕ from a few basic postulates: (1) The observed stationary states of ϕ at 0 deg. and ± 180 deg. are modeled as point attractors. The dynamics are then assumed to be purely relaxational. This is a minimality strategy in which only the observed attractor type (point attractor) appears in the model. (2) The model must reproduce the observed bifurcation diagram (i.e., bistable in a certain parameter régime, monostable in another parameter régime). (3) Pursuing again a minimality strategy, only the point attractors of the bifurcation diagram should appear. (4) Due to the angular character of ϕ the dynamics have to be 2π-periodic. (5) From the left-right symmetry found in the data, the model is required to be symmetric under the transformation $\phi \to -\phi$. The most general model obeying (1) to (5) is:

$$\dot{\phi} = -\frac{\mathrm{d}V(\phi)}{\mathrm{d}\phi} \tag{1}$$

where

$$V(\phi) = -a\cos(\phi) - b\cos(2\phi) \tag{2}$$

(cf. [8]). This is an explicit model of the dynamics of the relative phase with two parameters, a and b. Haken, Kelso and Bunz ([8], Fig. 5) show that equations (1) and (2) indeed capture the bifurcation diagram which has minima at $\phi = 0$ and $\phi = \pm 180$ deg. for $a/b < 4$ with the latter minimum turning into a maximum for $a/b > 4$. The order parameter dynamics (1) and (2) for ϕ can be derived from nonlinear oscillator equations for the two hands with a nonlinear coupling between them ([8]). We shall postpone discussion of the individual component's dynamics to Section 7.

A chief strategy of the foregoing dynamical analysis is to map the reproducibly observed states of the system onto attractors of a corresponding dynamical model. Thus, *stability* is a central concept, not only as a characterization of the two attractor states, but also because it is *loss of stability* that plays a chief role in effecting the transition. Stability can be measured in several ways. (1) If a small perturbation applied to a system drives it away from its stationary state, the time for the system to return to its stationary state is independent of the size of the perturbation (as long as the latter is sufficiently small). The "local relaxation time", τ_{rel}, (i.e., local with respect to the attractor) is therefore an observable system property that measures the stability of the attractor state. The smaller τ_{rel} is, the more stable is the attractor. The case $\tau_{\mathrm{rel}} \to \infty$ corresponds to a loss of stability.

(2) A second measure of stability is related to noise sources. Any real system described by low dimensional dynamics will be composed of, and be coupled to, many subsystems. These act to a certain degree as *stochastic forces* on the collective variables (cf. [1], Section 6.2 and references therein). The presence of stochastic forces and hence of *fluctuations* of the macroscopic variables, is not merely a technical issue, but of both fundamental and practical importance (cf. [1], Section 7.3 [28]). In the present context, the stochastic forces act as continuously applied perturbations and therefore produce deviations from the attractor state. The size of these fluctuations as measured, for example, by the variance or SD of ϕ around the attractor state, is a metric for the stability of this state. The more stable the attractor, the smaller the mean deviation from the attractor state for a given strength of stochastic force. Let us see how these stability measures behave in experiment.

4. Pattern change: loss of stability

Even cursory examination of typical experimental trajectories (see Fig. 1) reveals the presence of fluctuations. One may even suspect a non-trivial dependence on the control parameter frequency in that the relative phase plots look increasingly noisy near the transition (critical fluctuations?) as well as slower in returning from deviations (critical slowing down?). The task, then, is to test these features rigorously.

4.1. *Critical Fluctuations*

The mean relative phase and its standard deviation were calculated for each frequency plateau (and averaged over ten runs). Figure 2 shows the results for a typical subject.

The mean relative phase stays roughly constant if parameter scaling begins in the in-phase mode, but exhibits a transition if scaling starts in the anti-phase mode. A striking feature is the enhancement of fluctuations (as measured by SD) in the anti-phase mode before and during the transition. In contrast, a roughly constant level of fluctuations is observed in the in-phase mode. We draw the reader's attention especially to the enhanced SD on the pre-transitional plateau, where the system is still stationary (cf. [3, 6]). This provides experimental evidence for the presence of critical fluctuations and a quantitatively consistent fit between data and theory (within the limits of precision in such an approach, see [9] and Section 5).

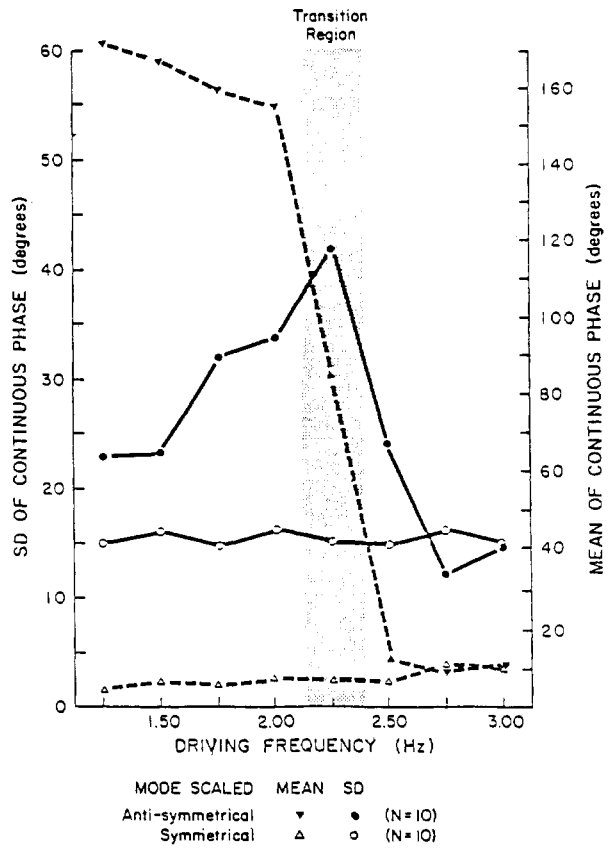

Fig. 2. The average mean relative phase modulus for the in-phase (open triangle) and anti-phase (closed triangle) modes of coordination and the average SD (in phase = open circles, anti-phase = closed circles) as a function of driving frequency (in Hz) for a set of 10 experimental runs. On a given run, the mean and SD were calculated for the last 3 s (600 samples) at a given frequency (from [6]).

4.2. *Critical slowing down*

Direct evidence of critical slowing down has been obtained from perturbation experiments carried out recently by Scholz [10] as part of his Ph.D. dissertation under the direction of the first author. The basic experiment involved perturbing one of the index fingers with a torque pulse (50 ms duration) as subjects performed in the two basic coordinative modes [11]. The apparatus consisted of a freely rotating support for each index finger that allowed flexion and extension about the metacarpophalangeal joint in the horizontal plane (see [12] for description). Electronics provided for the direct transduction of position, velocity and acceleration, and for the application of a predetermined magnitude of torque to either of the index fingers. In Scholz's experiment, only the right index finger was perturbed at random times during a trial and the torque onset was electronically timed to the peak flexion velocity of that finger. Torque magnitude was set individually for each subject in order to produce readily observable displacement of the finger into extension. Subjects ($N = 5$) were asked to move their fingers rhythmically in one of two modes of coordination: in-phase (relative phase $\approx$ 0 deg.), and anti-phase (relative phase $\approx$ 180 deg.). Scaling trials consisted of increasing the frequency of oscillation in nine 0.2 Hz steps every 10 sec starting at 1.0 Hz. When scaling began in the anti-phase mode of coordination a transition invariably occurred to the in-phase mode.

Relaxation time was operationally defined as the time from the offset of the perturbation until the continuous relative phase – calculated from the difference between each hand's phase plane trajectory – returned to its previous steady-state value. Except for the lowest movement frequencies (e.g., 1.0 to 1.2 Hz), relaxation time of the anti-phase

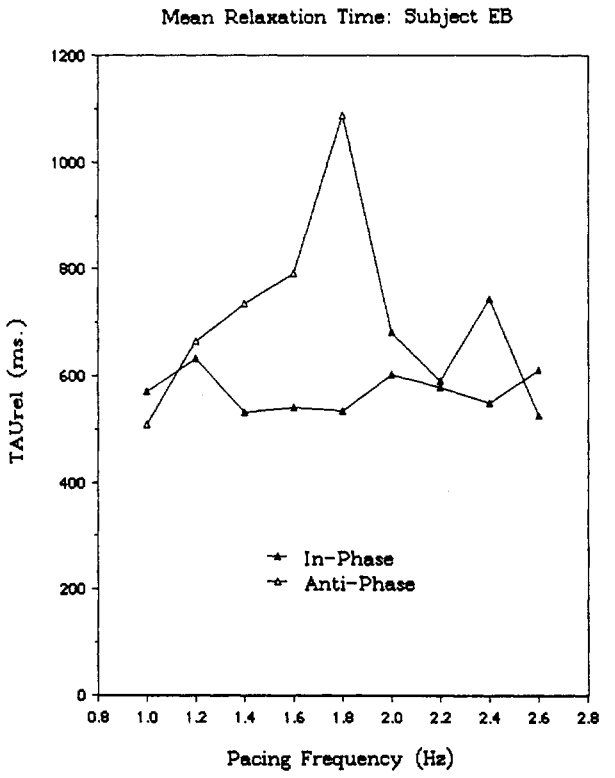

Fig. 3. The mean relaxation time (in ms) as a function of pacing frequency for the two coordinative modes, in-phase (closed triangles) and anti-phase (open triangles). Most of the transitions occur for this subject at 1.8 Hz. Each triangle contains at least 10 observations.

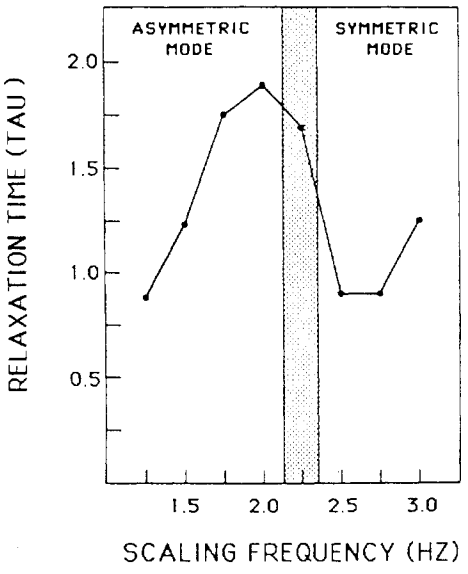

Fig. 4. Plot of mean relaxation time, calculated as the inverse of the line width of the power spectra of relative phase at half-power, versus the scaling frequency. One subject's data averaged across 10 trials. Power spectra calculated for 3 s of data (600 points) on each trial at each value of the scaling frequency.

mode was significantly longer than that of the in-phase mode for all five subjects. Furthermore, as the critical frequency for mode transition was approached, the relaxation time increased monotonically. The result is revealed by a significant positive correlation between the pacing frequency and relaxation time up to the transition ($p < 0.001$). No such increase occurred when scaling was carried out over the same frequency range beginning in the in-phase mode. Here, either no relationship existed between pacing frequency and relaxation time ($N = 3/5$), or relaxation time actually decreased with increasing frequency of movement ($N = 2/5; p < 0.001$). The results of one of the subjects are presented in Fig. 3.

Additional, though more preliminary evidence for critical slowing down has also been found (see [13]). The method for determining relaxation time in this case uses the power spectrum of the continuous relative phase calculated for the stationary portion of each frequency plateau. Due to the Wiener–Khinchin theorem, this function is just the Fourier transform of the relative phase autcorrelation function. It has a low frequency peak that reflects the relaxational dynamics of relative phase. Stochastic theory (see [9]) tells us that the line width of this low frequency peak is a measure of relaxation rate (the reciprocal of relaxation time). Figure 4 is a plot of relaxation time, τ_{rel}, as determined from the line width of the power spectrum of relative phase for one subject (the same data as shown in Fig. 2).

The strong enhancement of τ_{rel} before the transition can be clearly seen. Nevertheless, a lot of work remains to be done on this topic. An algorithm for determining the line shape of the relative phase spectral density function has to be developed. Detailed modelling is necessary to compare theory and experiment with respect to relaxation time in a quantitative fashion.

5. Stochastic model of the phase transition

With respect to the previously discussed features of the phase transition the model (1), (2) is as yet incomplete because it lacks a representation of fluctuations. Including fluctuations in the model allows us to: (1) test the consistency of the dynamical model experimentally (via time scales relations); (2) determine model parameters quantitatively; and (3) make non-trivial predictions that can be further tested experimentally. The latter point aims at finding lawful relations on the level of dynamics rather than a mere redescription of observations.

To account for fluctuations, and again guided by several reasonable assumptions, we add a stochastic force to eq. (1). We assume: (1) the source of the noise consists of many, weakly interacting degrees of freedom (e.g., on the neuromuscular level); (2) the noise sources are correlated over short times compared to the observed macroscopic dynamics (otherwise they are included in the deterministic part of equation (1)); and (3) the noise sources are regular during the transition. These assumptions imply that stochastic forces can be modeled as additive, gaussian, white noise ξ_t:

$$\dot{\phi} = -\frac{dV(\phi)}{d\phi} + \sqrt{Q}\,\xi_t \tag{3}$$

with

$$\langle \xi_t \rangle = 0; \quad \langle \xi_t\, \xi_{t'} \rangle = \delta(t - t') \tag{4}$$

where the parameter Q measures the noise strength [9]. This stochastic model is still incomplete, however. In order to solve eq. (3) and compare its solution to experimental data, we have to furnish initial conditions. Finding the appropriate initial conditions requires a discussion of several relevant *time scales* of the present system. Because this is an important point for modeling biological dynamics in many situations, we will be somewhat more general here.

To characterize the state of a biological system within a stochastic dynamical description three types of time scales are relevant. The first is the typical time scale on which the system is *observed*, τ_{obs} (i.e., how long the experimeter observes the system in a given preparation). The second is the previously discussed local relaxation time τ_{rel} (cf. Section 3), that is specific to a given attractor. The third one is the so-called *equilibration time* (or global relaxation time), τ_{equ} which is defined as the time it takes the system to achieve the stationary probability distribution from a typical initial distribution. In a bistable situation like ours, below the transition τ_{equ} is determined mostly by the typical time it takes to cross the potential hill (see, e.g., [14]).

If these time scales fulfill the following relation

$$\tau_{rel} \ll \tau_{obs} \ll \tau_{equ} \tag{5}$$

then the interpretation of observed states as attractor states is consistent. That is, the system has relaxed to a stationary state on the observed time scale, but is not yet distributed over all coexisting attractors according to the stationary probability distribution. When stationary states in an experiment are referred to, what is meant is that the time scale relation (5) is obeyed.

It is important to realize that much of the work in dynamical modeling of biological systems uses deterministic models only and thus implicitly makes the assumption that (5) holds (see, for instance, the contributions to the 1982 Conference on Nonlinearities in Brain Function [15] for typical examples). To neglect fluctuations and assume (5) throughout is dangerous, however, because (a) the relation (5) breaks down at critical points; (b) fluctuations are an important feature of

bifurcation phenomena, and (c) fluctuations are essential in bringing about transitions. Let us examine these three points in more detail.

In our system (3), as the transition is approached (i.e., the anti-phase mode loses its stability), the local relaxation time (with respect to the anti-phase mode) increases, while the global relaxation time decreases (because the potential hill between 0 and 180 deg vanishes). At the critical point both are of the same order as the observed time and one can see the transition. Thus, at the transition point, the time scales relation (5) is violated and an additional time scale assumes importance, namely the *time scale of parameter change*, τ_p. This reflects the fact that in our system (as often in biological systems) the control parameter that brings about the instability is itself changed in time. The relation of the time scale of parameter change to the other system times plays a decisive role in predicting the nature of the phase transition. If, for example,

$$\tau_{rel} \ll \tau_p \ll \tau_{equ} \tag{6}$$

then the system changes only as the old state actually becomes unstable. This transition behavior is sometimes referred to as a *second order phase transition* (because of an analogy with equilibrium phase transitions, see [1], Section 6.7). In that case features of critical phenomena (such as critical fluctuations or critical slowing down, see below) are predicted. If, on the other hand

$$\tau_{rel} \ll \tau_{equ} \ll \tau_p \tag{7}$$

then the system, with overwhelming probability, always seeks out the lowest potential minimum. It therefore switches state before the old state actually becomes unstable. Jumps and hysteresis (among other features) are generally predicted. This behavior is also called a *first order transition*, again in reference to equilibrium phase transitions [Note: In catastrophe theory, these two different transition behaviors are sometimes referred to as conventions, although they can, of course, be derived from the experimentally accessible relations (6) and (7). It is the failure to treat fluctuations that renders catastrophe theory incomplete in this respect].

Following these more general remarks, let us return to the concrete stochastic model (3). Because τ_p and τ_{obs} are of the same order in the experiment, we expect time scales relation (6) to hold up to the transition. At the transition all time scales may then be of the same order. This requires us to differentiate two parameter régimes: (a) The noncritical regime, where the system is stationary in the sense of (5); and (b) The critical régime, where the system exhibits transient behavior. In these régimes one can now solve the stochastic equation (3) via the corresponding Fokker–Planck equation ([9]). For the noncritical régime, stationary probability distributions of local models (that have only one stationary state at either 0 or 180 deg.) can be determined. From these the standard deviation (SD) as a measure of the width of the distribution can be calculated. As the transition is approached, the SD of the local model of the anti-phase mode increases, reflecting the enhancement of fluctuations. Using the experimental information on the local relaxation time and the SD in the noncritical régime, one can determine all model parameters a, b, and Q ([9]). In the critical régime the full Fokker–Planck equation can now be solved numerically, using an appropriate distribution from the pre-transitional

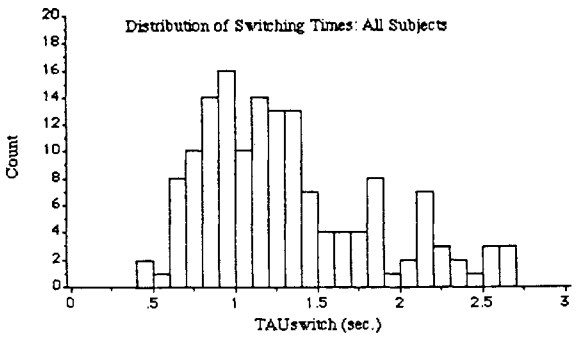

Fig. 5. The distribution of switching times for all subjects in Scholz's phase transition experiment (see text for details).

régime as an initial condition. Without further adjustable parameters the model accounts nicely for the transient behavior [9].

The stochastic model contains another feature that can be compared with experiments. This is the duration of the transient from the anti-phase state to the in-phase state – which we call the *switching time*. The basic idea is that during the transition the probability density of relative phase – initially concentrated at $\phi \approx \pm 180$ deg flows to $\phi \approx 0$ deg and accumulates there until the "new" peak at $\phi \approx 0$ deg is dominant and stationary. The model predicts the duration of this process both in terms of its distribution and its mean [9]. These switching times have been extracted from the experimental data described in Section 4.2 above. In most cases they were easy to calculate as the time between the relative phase value immediately before the transition and the value assumed immediately following the transition. The distribution of switching times for all five subjects is shown in Fig. 5. The match between theoretical prediction (cf. [9] Fig. 11) and empirical data is impressive, to say the least, even to the shapes of the switching time distributions. This new aspect is particularly interesting, because it shows that the switching process itself is quite closely captured by the stochastic dynamics of (3). Using the language of phase transitions may thus be adequate to understand the present phenomenon – even beyond the more superficial level of analogy.

6. Phase-locked modes: the "sea gull effect"*

In our discussion so far we have always assumed that the system has only two phase-locked patterns – in-phase and anti-phase – at its disposal. Is this assumption really valid? The experiments described in Sections 2 and 4 probe only these two states and their local environment (local in relative phase).

We shall now discuss experiments [16, 17], that allow us to establish the stabilities of all relative phase values, thus affording a view of the whole "potential landscape".

In Tuller and Kelso's experiment [16], the subject's task was simply to tap with the left index finger every time a light for the left hand flashed, and to tap with the right index finger every time a light for the right hand flashed. The set of

* The reason we dub this the "sea gull effect" is obvious from the shape of the function shown in Fig. 6 (bottom). Perhaps our proximity to the Atlantic Ocean played a role in naming it the way we did (for another example, see [17], Fig. 2).

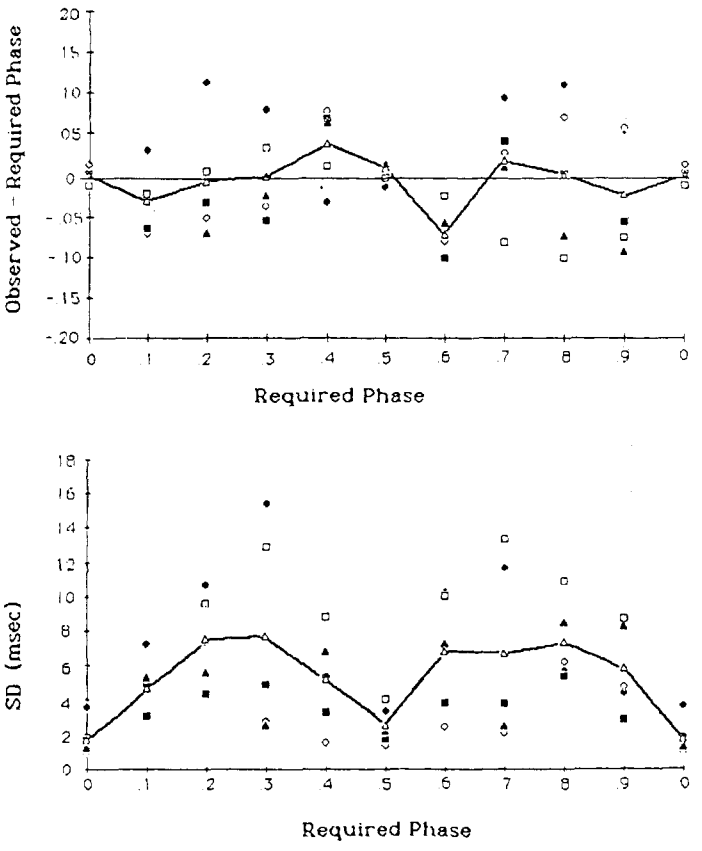

Fig. 6. Top. The phase of the pacing lights specifying the required phase plotted against the mean difference between the phase required and the phase actually produced. A negative number means that the required phase was underestimated. Each symbol represents an individual subject's mean computed over $N > 80$ movements *Bottom.* Standard deviation of the phase produced plotted against the required phase. Symbols same as above.

conditions involved different lag times between onsets of the two lights varying in 100 ms steps from synchrony to a 500 ms lag (or 0.5 out-of-phase) and back to synchrony. The cycle time for the lights was constant at 1 sec. The phases of the lights did not change within a trial. Four 24-sec trials of each of ten phase conditions were presented randomly.

The top portion of Fig. 6 shows the mean deviation from required relative phase as a function of the required phase difference. The bottom portion of Fig. 6 shows the standard deviation (SD) of the observed relative phase between the hands as a function of the required relative phase. The different symbols refer to different subjects and the open triangles connected by straight lines are the means across subjects. Obviously in-phase (at zero) and anti-phase (at 0.5) movements are the most stably produced. (This is the case in both musicians and non-musicians as well as in split-brain patients [16]). Moreover, the top portion of Fig. 6 shows how these two states attract neighboring states – the difference between observed and required phase passes through 0.0 and 0.5 with a negative slope. These findings are highly consistent with our basic modeling assumption, namely, that in-phase and anti-phase are the two basic stable phase-locked patterns. To make the implications of this experiment more stringent, however, we have to generalize our model to include the externally imposed required phase. A simple way to include the external pacing in the equation (3) for relative phase is to alter the potential. The potential (2) represents the system's intrinsic cooperativity. We assume that this remains valid under the paced conditions. Thus, we represent the required phase by adding a term to the potential that attracts the 'intrinsic' relative phase toward the required phase. The simplest function that does this (while conforming to certain periodicity requirements, see [18] for details) is $\cos[(\phi - \psi)/2]$, where ψ is the required phase.

The new potential thus reads:

$$V_\psi(\phi) = -a\cos\phi - b\cos(2\phi) - c\cos\left(\frac{\phi-\psi}{2}\right). \quad (8)$$

(Note that the new term breaks the $\phi \to -\phi$ symmetry as the pacing does in the experiment). The zeros of this potential are the new stationary states. [Unfortunately the corresponding transcendental equation cannot be solved analytically. We determined the stationary states numerically, using for parameters a and b values similar to those previously established to account for experimental data [9], and choosing c sufficiently large to see an effect of the new term. No systematic attempt to optimize parameters has yet been made, however.] In the top portion of Fig. 7 the deviation of the stationary solution for relative phase from the required phase ($\phi_{stat} - \psi$) is plotted as a function of required phase, ψ. Obviously our model captures the attractivity of the two basic modes. To determine the stochastic properties we proceed as in the previously discussed case of noncritical properties for the model (3) (cf. Section 5; [9]): Expanding the potential about its stationary solution and determining the stationary probability distribution of the resulting local model allows us to calculate the SD in this approximation. The bottom portion of Fig. 7 shows the SD as a function of required phase ψ (where a, b and c are as in the top portion and Q is chosen as in the model for the phase transition [9]). Obviously this function captures the qualitative features of the experimental data (although it is a somewhat edgy "see gull"!). Our modeling here acquires additional credibility through the fact that the potential (8) can again be derived from a model of the oscillatory components of the system, in which the external pacing has been incorporated. This is briefly discussed in the

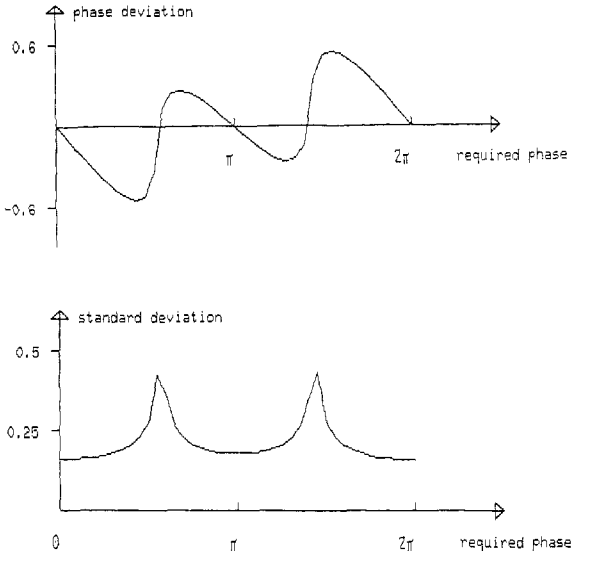

Fig. 7. Top: The deviation of relative phase from required phase as a function of required phase as calculated from the minima of V_ψ [eq. (8)]. The parameters were $a = 1$ Hz, $b = 1$ Hz, $c = 20$ Hz. *Bottom*: The standard deviation as determined from a local model around the minima of V_ψ. The parameters a, b, c were as above and $Q = 0.5$ Hz.

following section. A more detailed analysis of these models will be published elsewhere [18]. In summary, the global stability measurement performed in this experiment together with a theoretical model shows the consistency of our conceptual approach. We consider this continued close match of theory and experiment to be quite remarkable.

7. Modeling the subsystems

A key feature of the approach thus far has been to characterize coordinated states entirely in terms of the dynamics of macroscopic, collective variables (in this case relative phase is an order parameter). Here we address the nature of the subsystems themselves and how these can be coupled so as to produce coordinated states. We start at the next level down, as it were, which is the individual hands themselves. Experimentally, the behavior of the individual hands is observed as finger position x and velocity $\dot{x}$. The stable and reproducible oscillatory performance of each hand is modeled as an attractor in the phase plane $(x, \dot{x})$, in this case a limit cycle. Several experimental features constrain the modeling. Kinematic relationships, such as those between amplitude, frequency and peak velocity, have been measured ([19]). Figure 8 (from [19]) shows the amplitude-frequency relation for oscillatory movements of only one hand. The observed monotonic decrease of amplitude with frequency can be modeled by a combination of the well-known van der Pol and Rayleigh oscillators [8, 19]:

$$\ddot{x} + f(x, \dot{x}) = 0 \tag{9}$$

with

$$f(x, \dot{x}) = \alpha\dot{x} + \beta\dot{x}^3 + \gamma\dot{x}x^2 + \omega^2 x. \tag{10}$$

In mapping the observed oscillatory state onto a limit cycle the notion of stability is, once again, a key feature of our theory. This can again be tested by measuring the relaxation time after a perturbation of the hand in a fashion similar to that described in Section 4. Such experiments have been recently performed by Kay under the direction of the first author ([20]). Along with the observed kinematic relations, relaxation time measures allow one to determine all parameters in eqs. (9) and (10).

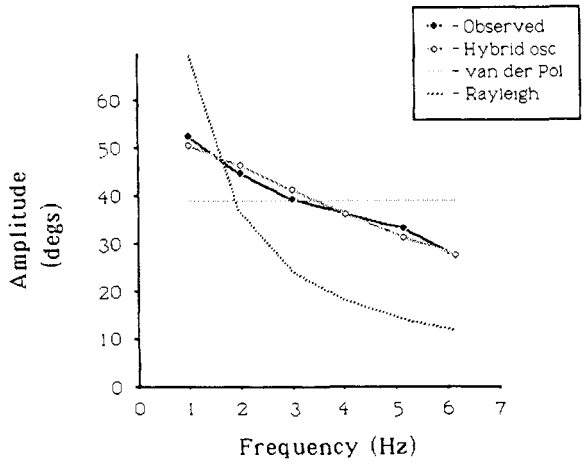

Fig. 8. Amplitude versus frequency for rhythmical movements of a single hand. The experimental points (full circles) are means over subjects, experimental sessions and trials. The (hybrid) oscillator of eqs. (9) and (10) was fitted to the data (least squares). For illustration purposes fits of the van der Pol and the Rayleigh oscillators alone are also shown.

Another assumption implicit in eqs. (9) and (10) is that the oscillation is essentially autonomous. This can be experimentally tested in the perturbation paradigm by phase resetting techniques (see, e.g., [21]). The basic idea is that the phase of an autonomous oscillator is marginally stable, unlike that of a driven oscillator which is locked to the driving function. This assumption has also been checked in Kay's experiment. Preliminary results show that the oscillation is indeed autonomous (in the absence of external pacing).

How can the components with their dynamics (9) and (10) give rise to the phase-locked coordinative modes? Obviously their dynamics have to be coupled. Haken, Kelso and Bunz [8] have determined coupling structures that can account for the observed phase-lockings. The simplest model that achieves this is a van-der-Pol-like coupling of the form:

$$\ddot{x}_1 + f(x_1, \dot{x}_1) = (\dot{x}_1 - \dot{x}_2)\{A + B(x_1 - x_2)^2\} \tag{11}$$

$$\ddot{x}_2 + f(x_2, \dot{x}_2) = (\dot{x}_2 - \dot{x}_1)\{A + B(x_2 - x_1)^2\} \tag{12}$$

where f is the oscillator function (10) and A and B are coupling constants. The experimental observation, that the kinematic relations (e.g., amplitude–frequency relation) are not significantly different between the coordinative modes and the single hand movements show that the coupling constants A, B are small compared to the corresponding coefficients α, γ of the oscillator function (10) [19]. In spite of this the coupling structure (11) and (12) gives rise to the two phase-locked states. Indeed Haken, Kelso and Bunz [8] were able to derive the equation for relative phase (1), (2) from eqs. (11) and (12) using the slowly varying amplitude and rotating wave approximations. These results not only provide further support for the dynamical model on the collective variable level, but also establish in a rigorous fashion the relation of the two levels of description.

Finally, we indicate briefly how the pacing of both hands in the "sea-gull effect" (Section 6) may be incorporated into the model at the component level. The basic idea is similar to that used to determine the potential (8): We assume that the system's intrinsic dynamics are still intact and the pacing acts as an additional external force. For the oscillator equations this can be done by adding a periodic driving force to their oscillator function, e.g., as

$$\ddot{x}_1 + f(x_1, \dot{x}_1) = (\dot{x}_1 - \dot{x}_2)\{A + B(x_1 - x_2)^2\} + F\cos(\omega t), \tag{13}$$

$$\ddot{x}_2 + f(x_2, \dot{x}_2) = (\dot{x}_2 - \dot{x}_1)\{A + B(x_2 - x_1)^2\} + F\cos(\omega t + \psi). \tag{14}$$

Here F is the coupling constant of the driving force and ψ the required relative phase. For convenience we have chosen the natural frequency of the oscillators as identical to the driving frequency. In fact, the ability of the subjects to entrain their rhythmic movements without a phase lag to the external pacing lights is an interesting subject in its own right and deserves further theoretical and experimental study. Using again the slowly varying amplitude and the rotating wave approximations we were able to derive the following equations for the relative phase ϕ and the phase sum θ:

$$\dot{\phi} = -\frac{\partial V(\phi, \theta)}{\partial \phi} \tag{15}$$

$$\dot{\theta} = -\frac{\partial V(\phi, \theta)}{\partial \theta} \tag{16}$$

with a potential:

$$V(\phi, \theta) = -a \cos \phi - b \cos 2\phi - c \sin\left(\frac{\theta - \psi}{2}\right) \cos\left(\frac{\phi - \psi}{2}\right) \quad (17)$$

where

$$a = -A - 2Br_0^2, \quad b = \tfrac{1}{2}Br_0^2 \quad \text{and} \quad c = F/(\omega r_0)$$

with amplitude

$$r_0 = \sqrt{\alpha/(3\beta\omega^2 + \gamma)}.$$

If one assumes the phase sum to have relaxed to its stationary value $\theta = -\pi + \psi$ the resulting equation for relative phase is exactly:

$$\dot{\phi} = -\frac{dV_\psi(\phi)}{d\phi} \quad (18)$$

with the potential V_ψ of eq. (8). Thus again we have derived the collective variable dynamics from the component level. The details of these calculations will be published elsewhere ([18])

8. Conclusions: "Phenomenological Synergetics

The laws governing the dynamic patterns produced by complex, biological systems that possess very many degrees of freedom (such as the human brain which has $\sim 10^4$ neurons and neuronal connections) are, in general, not known. Unlike certain physical systems, the path from the microscopic dynamics to the collective order parameters – as in Haken's *slaving* principle – is not readily accessible to theoretical analysis. Here we suggest that an understanding of biological order may still be possible via an alternative approach, namely one in which the nature and dynamics of the (low-dimensional) order parameters are first empirically determined, particularly near nonequilibrium phase transitions (or bifurcations). Then the relevant subsystems and their dynamics can be identified. This approach, which we may call "phenomenological synergetics", has provided the conceptual framework for the empirical studies of spatiotemporal order in bimanual coordination that we have reported here. Parenthetically, we have preliminary, but exciting evidence that the approach is useful for understanding another system, namely the multiple articulator movements that structure the sounds of speech ([7]). A similar strategy has been successfully applied to "muscle streaming" by Shimizu and Haken [22, 23].

"Understanding" is sought, in the present approach, not through some privileged scale of analysis, but within the abstract level of the essential (collective) variables and their dynamics, *regardless of scale or material substrate.* Not only may the language of dynamics be appropriate at the behavioral level (e.g., in the patterns among muscles and kinematic events), but also, we hypothesize, at the more microscopic scale of neurons and neuronal assemblies. Many of the dynamical features we have observed and modeled in our experiments, for example, synchronization, phase-locking, switching, etc., can also be observed in the neuronal behavior of even the lowliest creatures, e.g., in the buccal ganglion of the snail, *Helisoma* (as in Kater and colleagues' work, cf. [24] for review) or in the motoneuronal firing patterns of *Pleurobranchaea* during feeding (cf. [25]). Thus the long sought-for link between neuronal activities (microscopic events) and behavior (macroscopic events) may actually reside in the coupling of dynamics on different levels (cf. Section 7 above). Relatedly, the classical dichotomy in biology between structure and function may be one of appearance only. The present theory promotes a unified treatment, with the two processes separated only by the time scales on which they live.

Finally, we want to stress – after Bridgeman [26] and Haken [27] – the operational nature of the present approach. That is, dynamics are formulated for observable variables only and predictions are made that can be experimentally tested. As much as possible, a minimality strategy is followed in which all consequences of a theoretical formulation are checked for their empirical validity. Insight is not necessarily gained by increasingly accurate quantitative descriptions of data, or by using increasingly complicated dynamical equations. Rather, we seek to account for a larger number of experimental features with a smaller number of theoretical concepts.

Acknowledgements

The work reported here was supported, in large part, by Contract No. N00014-83-K0083 from the U.S. Office of Naval Research (H. Hawkins, Scientific Officer) and by NINCDS Grants NS-13617 and BRS Grant RR-05596. G. Schöner was supported by a Forschungsstipendium of the Deutsche Forschungsgemeinschaft, Bonn, FRG.

References

1. Haken, H., Synergetics: An Introduction, Springer-Verlag, Heidelberg (3rd ed) (1983).
2. Haken, H., Advanced Synergetics, Springer-Verlag, Heidelberg (1983).
3. Kelso, J. A. S. and Scholz, J. P., Cooperative Phenomena in Biological Motion, In H. Haken (Ed.): Complex Systems: Operational Approaches in Neurobiology, Physical Systems and Computers, Springer-Verlag, Berlin, (1985).
4. Kelso, J. A. S., Bulletin of the Psychonomic Society **18**, 63 (1981).
5. Kelso, J. A. S., Am. J. Physiol.: Reg. Int. Comp. Physiol. **15**, R1000 (1984).
6. Kelso, J. A. S., Scholz, J. P., and Schöner, G., Phys. Lett. A (in press).
7. Kelso, J. A. S., Saltzman, E. L., and Tuller, B., J. Phonetics **14**, 29 (1986).
8. Haken, H., Kelso, J. A. S., and Bunz, H., Biological Cybernetics **51**, 347 (1985).
9. Schöner, G., Haken, H., and Kelso, J. A. S., Biological Cybernetics **53**, 247 (1986).
10. Scholz, J. P., Ph.D Dissertation, University of Connecticut, Storrs, CT. (1986).
11. Kelso, J. A. S., Holt, P. G., Rubin, P., and Kugler, P., J. Motor Behav. **13**, 226 (1981).
12. Kelso, J. A. S. and Holt, K. G., J. Neurophysiology **43**, 1183 (1980).
13. Kelso, J. A. S., Schöner, G., Scholz, J. P., and Haken, H., Nonequilibrium Phase Transitions in Coordinated Movement Involving Many Degrees of Freedom, In: Perspectives in Biological Dynamics and Theoretical Medicine, Annals of the New York Academy of Sciences (in press).
14. Gardiner, C. W., Handbook of Stochastic Methods for Physics, Chemistry and the Natural Sciences, Springer-Verlag, New York (1983).
15. Garfinkel, A. and Walter, D. O. (Eds.), Am. J. Physiol.: Reg. Int. Comp. Physiol. **14**, R450 (1983).
16. Tuller, B. and Kelso, J. A. S., Coordination in Normal and Split-Brain Patients, Paper presented at *Psychonomic Society*, Boston, MA. (1985).
17. Yamanishi, J., Kawato, M., and Suzuki, R., Biological Cybernetics **37**, 219 (1980).
18. Schöner, G., Kelso, J. A. S., and Tuller, B. (forthcoming).
19. Kay, B. A., Kelso, J. A. S., Saltzman, E., and Schöner, G., J. Exp.

Psych. Human Perception and Performance (in press).
20. Kay, B. A., Ph.D Dissertation, University of Connecticut, Storrs, Conn. (1986).
21. Winfree, A. T., The Geometry of Biological Time, Springer-Verlag, New York (1980).
22. Shimizu, H., In Haken, H. (Ed.), Evolution of Order and Chaos in Physics, Chemistry and Biology, Springer-Verlag, Berlin, Heidelberg, New York (1982).
23. Shimizu, H. and Haken, H., J. Theoret. Biol. **104**, 261 (1983).
24. Kater, S. B., Dynamic Regulators of Neuronal Form and Connectivity in the Adult Snail Helisoma, In: Model Neural Networks and Behavior (Edited by Allen I.), Selverston, Plenum (1985).
25. Mpitsos, G. J. and Cohan, C. S., J. Neurobiology (in press).
26. Bridgeman, P. W., The Nature of Physical Theory, Dover Pub. (1953).
27. Haken, H., Operational Approaches to Complex Systems. An Introduction, In: Haken, H. (Ed.). Complex Systems – Operational Approaches in Neurobiology, Physics and Computers, Springer-Verlag, Berlin, Heidelberg, New York (1985).
28. Landauer, R. and Woo, J. W. F., In Rice, S. A., Freed, K. F. and Light, J. C., Statistical Mechanics: New Concepts, New Problems, New Applications, University of Chicago Press, Chicago, 1972.

Notes added in proof

1. Regarding the experiments described in Section 2, Professor H. Swinney (University of Texas, Austin) has inquired about additional bifurcations. In fact, as frequency is scaled to even higher values, a further bifurcation has been observed (cf. [3]) in which the fingers shift from a symmetrical abduction-adduction pattern to a symmetrical flexion-extension pattern (see [3] Fig. 10 and Sect. 6.7). We do not discuss this bifurcation further here, however, because it has not been studied in any detail as yet. Nevertheless, the increase in mean relaxation time at 3 Hz seen in the present Fig. 4 may be because this new bifurcation is observed near that value.

2. The analogy of the observed transition with equilibrium second order phase transitions refers to the presence of critical fluctuations and critical slowing down. The origin of these critical phenomena in the present case, however, is different from the equilibrium situation. In particular, symmetry breaking does not occur. It is only due to the time scales relation (6) that criticality is seen in what one might rather call – following a suggestion of Professor R. Landauer (IBM) – a limiting case of a first order transition. We would like to thank Profs. Swinney and Landauer for raising these points with us.